Report to the Clerk Maxwell Cancer Research Fund, October 2009
Prof C Simon Herrington, University of St Andrews.

Optical Imaging for Cancer Diagnosis

Our work focuses on the use of Raman spectroscopy for cancer diagnosis and, in addition to the generous donation from the Clerk Maxwell Cancer Research Fund, is supported by Cancer Research UK, EPSRC and the Chief Scientist's Office. We have made progress in three specific areas. First, we have consolidated our earlier work on cells from cervical cancer by demonstrating that Raman spectroscopy can discriminate various stages of lung cancer development. This work has been published in the *International Journal of Cancer* (Jess et al, *Int J Cancer* 2009; 124: 376-380 – copy attached). Second, we have developed a novel technique involving wavelength modulation to reduce background signal, particularly that related to fluorescence, in Raman spectroscopy. Third, we have applied Raman spectroscopy to the analysis, and imaging, of formalin-fixed, paraffin-embedded clinical tissue samples.

Wavelength Modulation
Raman spectroscopy generates a spectral fingerprint that is both weak and masked by other optical effects, particularly fluorescence. Wavelength modulation aims to reduce these effects whilst retaining the Raman signal, thus enhancing signal-to-noise ratio and improving the applicability of this methodology to clinical material. The approach involves the acquisition of multiple short-duration spectra, each of which corresponds to a different known excitation wavelength. A tuneable laser is used to modulate its wavelength periodically and, by synchronising spectrum acquisition to the modulated laser, each excitation wavelength can be associated with a specific Raman spectrum. The differential spectrum is then retrieved using numerical approaches. We have successfully applied this approach to the analysis of polymer spheres, red blood cells and Chinese hamster ovary (CHO) cells. This work has been submitted for publication.

Raman imaging
Building on our experience with Raman spectroscopy of cells, we have begun to develop approaches for Raman interrogation of tissues, focusing specifically on formalin-fixed, paraffin-embedded tissue in the first instance to allow direct application to archival human tissues. We have applied this approach to the investigation of clinical samples from normal and abnormal cervical tissues and have been able not only to generate images from normal tissue structures but also to discriminate in this way between normal and abnormal epithelium. These findings suggest that Raman mapping has the potential to provide images that are useful for disease diagnosis. Our findings are of particular relevance to cervical screening pathology. This work has been submitted for publication.

Int. J. Cancer: **124,** 376–380 (2009)

Optical detection and grading of lung neoplasia by Raman microspectroscopy

Phillip R.T. Jess[1], Michael Mazilu[1], Kishan Dholakia[1], Andrew C. Riches[2] and C. Simon Herrington[2]*

[1]*SUPA, School of Physics and Astronomy, University of St. Andrews, North Haugh, St. Andrews, Fife, KY16 9SS, United Kingdom*
[2]*Bute Medical School, Bute Medical Buildings, University of St. Andrews, St. Andrews, Fife, KY16 9TS, United Kingdom*

The aim of this study was to investigate whether Raman spectroscopy could be used to identify and potentially grade lung neoplasia in cell samples. Normal human bronchial epithelial cells (HBEpCs) were analyzed by Raman spectroscopy and compared with (*i*) HBEpCs expressing human papillomavirus (HPV) type 16 E7 or CDK4; (*ii*) the immortalized bronchial epithelial cell line BEP2D and (*iii*) its asbestos-transformed derivative AsbTB2A. Overall, Raman spectroscopy, in combination with a linear discriminant analysis algorithm, was able to identify abnormal cells with a sensitivity of 91% and a specificity of 75%. Subdivision of the cell types into 3 groups, representing normal cells (HBEpCs), cells with extended lifespan (HBEpCs expressing HPV 16 E7 or CDK4) and immortalized/transformed cells (BEP2D and AsbTB2A) showed that Raman spectroscopy identifies cells in these categories correctly with sensitivities of 75, 79 and 87%, and specificities of 91, 85 and 96%, respectively. In conclusion, Raman spectroscopy can, with high sensitivity, detect the presence of neoplastic development in lung cells and identify the stage of this development accurately, suggesting that this minimally invasive optical technology has potential for lung cancer diagnosis.

Key words: lung; cancer; Raman; spectroscopy

Carcinoma of the lung is one of the most common cancers worldwide and is the leading cause of cancer mortality, with ~1.8 million deaths being reported each year.[1] The major risk factors for its initiation and promotion are smoking and exposure to industrial agents such as asbestos. Lung cancer has an age-adjusted 5-year survival rate of only 10%,[2] which is significantly lower than that of many other common cancers.[2,3] Thus, there is a pressing need for an objective screening technique that can identify early neoplastic changes and hence both improve lung cancer diagnosis and, consequently, reduce lung cancer mortality.

Methods currently employed in the detection of lung cancer include imaging modalities such as plain X-ray and CT scanning: sputum may also be examined for the presence of tumor cells. The presence of an abnormality normally leads to further investigation by bronchoscopy, at which a biopsy sample, or bronchial washings and brushings, are obtained to provide cellular material for examination. Although effective for detecting lung cancer, there is evidence that, although screening programs based on chest X-ray and sputum cytology lengthen survival, they have no impact on mortality rates from lung cancer.[4,5]

A great deal of effort has been focused on exploring new methods for lung cancer screening and detection. One of the most exciting avenues of research has been the investigation of optical approaches as they potentially offer minimally invasive, accurate and specific diagnosis. One of the most promising optical methods for the study of neoplasia is Raman spectroscopy, a vibrational scattering technique that has not only been successfully demonstrated to detect the earliest stages of neoplastic development, in a variety of organ systems,[6] but also offers the possibility of distinguishing the stages of tumor development.[7] Raman spectroscopy is a laser-based scattering spectroscopy and refers to scattered light, from a molecular or cellular sample, which displays a frequency shift that is associated with the energy of specific molecular vibrations within the sample of interest. This manifests itself physically as a shift in the wavelength of the photon, unique to the scattering bond, away from the incident wavelength. In this manner, it provides a detailed biochemical composition of the sample, giving a biochemical "fingerprint." The collection and examination of these shifted wavelengths result in the formation of a Raman spectrum that is a plot of energy shift away from the incident wavelength, usually measured in relative wavenumbers *versus* scattering intensity.

The application of Raman spectroscopy to cellular material could provide a screening tool for the identification of neoplastic changes in, for example, sputum samples. A small number of studies have demonstrated the potential of Raman spectroscopy to discriminate between normal lung tissue and tumors.[8–11] Raman spectroscopy has also been used to examine the intracellular carotenoid levels in lymphocytes retrieved from both healthy patients and those with lung cancer.[12] However, the ability of Raman spectroscopy to identify neoplastic changes in cells, similar to the material available from bronchial brushings, washings and sputum, has not been evaluated. Thus, in this study, we used cell lines representing the spectrum of lung neoplasia to test the hypothesis that Raman spectroscopy could discriminate normal cells from cells at various points on the pathway to malignant transformation.

Material and methods

Cell types, culture and preparation

Five cell types were chosen to represent the spectrum of neoplastic development in the lung. Primary normal human bronchial epithelial cells (HBEpCs, Promocell, Heidelberg, Germany) were used as normal cells and maintained in airway epithelial cell growth medium with supplements (Promocell). Retroviral transduction of HBEpCs was carried out as described previously[13,14] to produce HBEpCs expressing human papillomavirus (HPV) type 16 E7 (E7 cells) or CDK4 (CDK4 cells): transduced cells were selected in G418 at a concentration of 30 mg/ml. The packaging cell line PA317 containing wild-type HPV 16 E7 cloned into the pLXSN vector,[15] and the packaging cell line psi-CRIP containing wild type CDK4 cloned into the pBABE puro vector,[14] were maintained in Dulbecco's modified Eagle's medium containing 10% fetal calf serum or 10% calf serum, respectively.

The HPV18-immortalized human bronchial epithelial cell line BEP2D[16] and a malignant, transformed cell line derived from it following exposure of the cells to asbestos (chrysotile fibers), AsbTB2A,[17] were maintained in airway epithelial cell growth medium.

Cell suspensions from the 5 different cell types were harvested using trypsin/EDTA. The cells were then resuspended in medium containing serum and pelleted by centrifugation at 150 g for 5 min. They were resuspended in PBS, pelleted again and the pelleted cells fixed by suspension in 70% (v/v) ethanol. Cells were prepared for Raman analysis by again pelleting the cells and washing them in PBS to remove the ethanol. Finally, the cells were resuspended in a small volume of PBS.

Grant sponsors: Engineering and Physical Sciences Research Council, UK, Scottish Enterprise Fife, Clerk-Maxwell Cancer Research Fund.
***Correspondence to:** Bute Medical School, Bute Medical Buildings, University of St. Andrews, St. Andrews, Fife, KY16 9TS, United Kingdom. E-mail: csh2@st-andrews.ac.uk
Received 10 June 2008; Accepted after revision 1 August 2008
DOI 10.1002/ijc.23953
Published online 26 August 2008 in Wiley InterScience (www.interscience.wiley.com).

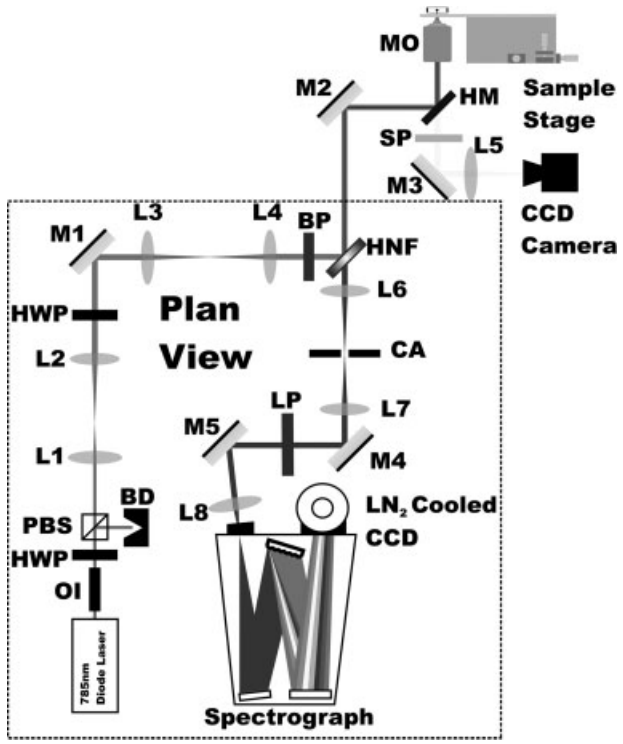

Figure 1 – Schematic of the confocal Raman microspectroscopy setup. Abbreviations are as follows: OI, optical isolator; HWP, half waveplate; PBS, polarizing beam splitter cube; BD, beam dump; L, lens; M, mirror; BP, band pass; HNF, holographic notch filter; HM, hot mirror; MO, microscope objective; SP, short pass; CA, confocal aperture; and LP, long pass.

Confocal Raman microspectroscopy

Confocal Raman microspectroscopy is the combination of confocal microscopy with traditional Raman spectroscopy. A home-built inverted Raman microspectroscopy system was constructed for this study (Fig. 1). Briefly, a temperature-stabilized laser diode (Sanyo DL-7140-201s) operating at 785 nm with a maximum output power of 80 mW is used as the source for the system. The laser beam is passed through an optical isolator, to ensure wavelength stability, and into a half waveplate polarizing beam splitter set that acts to adjust the optical power without affecting the wavelength. The beam is then expanded, *via* L1 and L2, and passed through a second half waveplate that can be used to adjust the polarization of the Raman scattered light. The beam is then reflected by mirror M1 into a relay lens set, L3 and L4, which can be used for beam steering and to adjust the focus of the laser in the sample chamber. The beam is passed through a bandpass filter (Semrock optics Max line 785), to remove any spontaneous emission from the laser source, and onto a 45° holographic notch filter (Tydex Notch-4) that reflects only a narrow band centered on the laser wavelength and passes all other wavelengths. The beam is then periscoped, *via* M2, into the inverted microscope and passed onto the hot mirror which reflects the beam into the microscope objective (Nikon Plan 50× oil immersion) that focuses the beam onto the sample. As the hot mirror passes visible wavelengths, the sample can be illuminated from above with incoherent light in order to image the sample on the CCD camera. The Raman scatter is collected by the same microscope objective and guided to the holographic notch filter, where it is passes through onto L6 which acts as a tube lens for the microscope objective forming an image on the confocal aperture. The confocal aperture is a 400-μm pinhole that defines an examination cylinder in the sample of diameter 8 μm and depth ~20 μm (calculated according to the method of Tabaksblat *et al.*[18]). Lens 7 is used to recollimate the Raman scatter, which is then steered into the spectrograph (Jobin Yvon iHr 550) *via* M4 and M5. A long pass filter (Semrock optics Razoredge 785) is used to suppress any remaining Rayleigh scatter. Finally, Lens 8 is used to reform the image at the entrance of the spectrograph, which separates the collected Raman scattering according to wavelength, and a liquid nitrogen-cooled CCD camera (CCD-2048×512-FIVS-3LS) is used to record the Raman spectra.

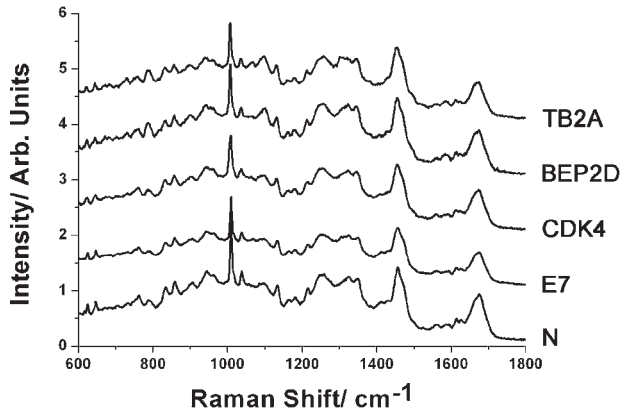

Figure 2 – Average spectra of the 5 cell types examined, offset for ease of viewing. N, normal human bronchial epithelial cells (HBEpC); E7, HBEpCs expressing HPV 16 E7; CDK4, HBEpCs expressing CDK4; BEP2D—BEP2D; and TB2A—AsbTB2A.

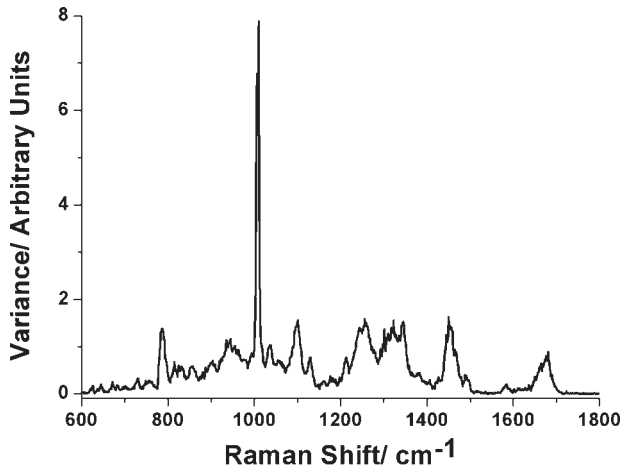

Figure 3 – Plot of variance, between the 5 cell lines, at each wavelength position on the Raman spectrum.

In total, single spectra and background readings were recorded from 75 cells from each population: the laser power at the cells was 50 mW and an integration time of 120 sec was sufficient to collect a good quality spectrum. During acquisition the laser was focused on the cell nucleus, as this is where most of the pertinent information is likely to originate, but with the generous confocal volume, a proportion of the cytoplasm and cell membrane is also likely to have been examined. No complete set of spectra, for any one cell type, was recorded sequentially. Furthermore, for each cell type, the cells analyzed were derived from several different cultures to ensure that any observed differences were the result of biological variations rather than variations in instrument background or cell culture techniques.

Spectral analysis and data treatment

Before commencing data treatment on the Raman spectra, background signal, consisting of the spectrum measured while the Raman excitation beam was focused next to the cell, was subtracted from

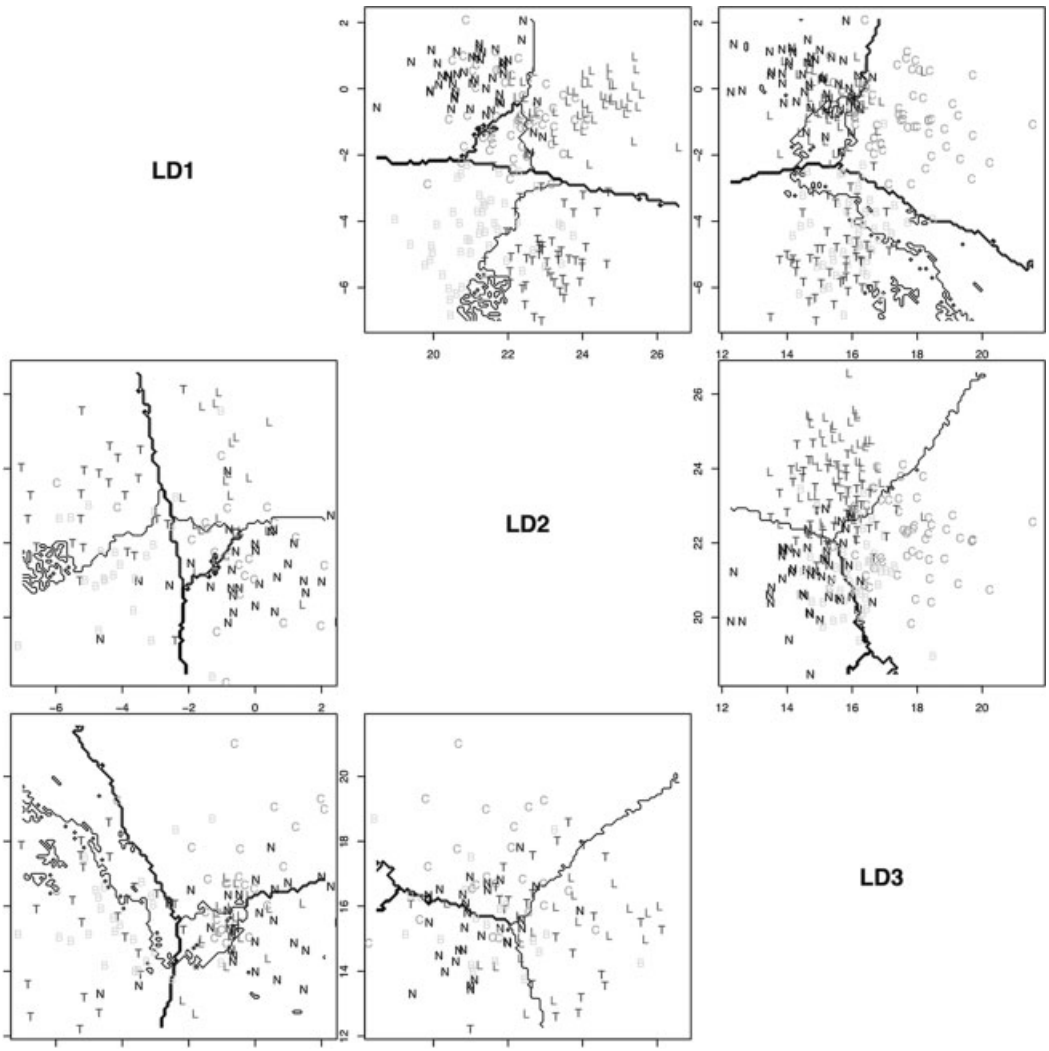

FIGURE 4 – Linear discriminant analysis. The top 3 figures show the training set distribution of the linear discriminant coordinates while the bottom 3 correspond to the cross-validation set used to calculate the confusion matrix. The axes are as follows: the horizontal axes in the first, second and third column are respectively the first, second and third linear discriminant coordinates while the vertical axes of the first, second and third row are the first, second and third linear discriminant coordinates. The contour lines correspond to the boundaries between the different cells where we used the k-nearest neighbors to decide on the classification distance. The "N," "L," "C," "B," "T" cells correspond in sequence to normal human bronchial epithelial cells (HBEpCs); HBEpCs expressing HPV 16 E7; HBEpCs expressing CDK4; BEP2D and AsbTB2A.

each individual spectrum. This subtraction removes most of the fluorescence generated by the optical system, cell surroundings and eliminates the dark current from the CCD detector. A Mathematica script was subsequently used to align the spectra to compensate for any small drifts in laser wavelength over the experimental period. Finally, the data were normalized according to the total intensity of each individual spectrum, that is, the area under the curve.

After the initial spectral treatment, the noise distribution of the individual CCD pixels was studied for each single cell type, and across different cell types. Quantile–quantile plots and histograms showed that the distributions were normal, but because the sample was relatively small local peaks in the histograms were observed. The normality improved when averaging across neighboring pixels and an optimum was achieved when considering 17 pixels for the average, giving an effective spectral resolution of 20 cm^{-1}. This optimum value was assessed through subsequent leave-one-out cross-validation of the models used.

To classify and build a predictive model based on the Raman spectra, we used linear discriminant analysis (LDA)[19] together with the k-nearest neighbors (k-NN) method. The LDA method searches for the projection that minimizes the variance between the spectra from the same cell type, while maximizing variance between different cell types. After finding the optimum projections for the LDA methods, we used only the first 4 main projection components for the predictive classification, which avoids over-fitting the model. These 4 projections were then used in conjunction with the k-NN method to classify the cross-validation data sets.

TABLE I – CONFUSION MATRIX GIVING THE PERCENTAGE CLASSIFICATION FOR EACH CELL TYPE

%LDA	N	E7	CDK4	BEP2D	TB2A
N	75	11	11	2	1
E7	16	77	5	4	4
CDK4	16	18	58	1	1
BEP2D	4	3	10	63	20
TB2A	0	5	4	21	70

Rows give the proportion of each cell type classified by linear discriminant analysis (LDA) as the cell types given in the columns. N, normal bronchial epithelial cells (HBEpCs); E7, HBEpCs expressing HPV 16 E7; CDK4, HBEpCs overexpressing CDK4; BEP2D, the BEP2D cell line; TB2A, the AsbTB2A cell line.

TABLE II – SUMMARY OF SENSITIVITIES AND SPECIFICITIES FOR THE IDENTIFICATION OF EACH CELL TYPE; FOR THE IDENTIFICATION OF CELLS WITH AN EXTENDED LIFESPAN (E7 OR CDK4); FOR THE IDENTIFICATION OF CELLS THAT ARE IMMORTALIZED OR TRANSFORMED (BEP2D OR TB2A) AND FOR THE IDENTIFICATION OF ALL ABNORMAL CELL TYPES (E7 OR CDK4 OR BEP2D OR TB2A)

	N	E7	CDK4	BEP2D	TB2A	Extended lifespan	Immortalized or transformed	All abnormal cell types
Sensitivity (%)	75	77	58	63	70	79	87	91
Specificity (%)	91	91	93	93	94	85	96	75

N, normal bronchial epithelial cells (HBEpCs); E7, HBEpCs expressing HPV 16 E7; CDK4, HBEpCs over expressing CDK4; BEP2D, the BEP2D cell line; TB2A, the AsbTB2A cell line.

The k-NN modeling considers the Euclidian distance between the linear discriminants of a cross-validation spectra and the training set. The classification is decided by the majority vote of the k-NN. These classifications are then collated in a confusion matrix, which gives the percentage of a cell-type *i* that is predicted in the cross validation process as cell-type *j*. The diagonal values of the confusion matrix give the percentage of correct predictive classification for the different cell types, and the average of these values gives the overall predictive efficiency of the method. We considered a random 2:1 split between training and validation sets, and the final confusion matrix results from an average of 300 of these confusion matrices built from the same experimental dataset.

Results

Good quality Raman spectra were acquired from all samples giving the resultant average spectra that can be seen in Figure 2. Visual interpretation of the average spectra is difficult for such a large variety of cell lines; however, examination of the variance between the 5 cell lines at each wavelength position provides some insight into which peaks vary most across the spectrum from normal to transformed cell lines. A plot of variance *vs.* wavelength (Fig. 3) shows that several peaks evolve across the cells and cell lines examined. From this plot, the most important peaks appear at 748, 1,009, 1,101, 1,256, 1,309, 1,343, 1,451 and 1,676 cm^{-1}: these are derived from DNA bases and backbone, proteins, amides and lipids. These features are consistent with the association of neoplastic progression with genomic and metabolic changes.

However, the main focus of this investigation was to determine if Raman spectroscopy can be used as a tool for detection of the onset of lung neoplasia. This requires objective comparison of the spectra and, hence, multivariate analysis was employed. Initially, 125 spectra, 25 from each cell type, were randomly excluded to be used later as a validation set and the remainder was used as a training set for the LDA algorithm. Once trained, the validation spectra were fed into the LDA model to determine its ability to correctly identify unknown spectra. The LDA charts for the training and validation sets are given in Figure 4, and the confusion matrix for the diagnosis of the validation set is presented in Table I. A summary of the sensitivities and specificities for the identification of each cell type is given in Table II.

Discussion

In this study, we have examined the ability of Raman spectroscopy to distinguish between cell types representing the spectrum of lung neoplasia. Raman spectroscopy, in combination with LDA, was able to correctly identify 75% of the normal human bronchial epithelial cells (HBEpCs), 77% of the HBEpCs expressing HPV 16 E7 (E7 cells), 58% of the HBEpCs expressing CKD4 (CDK4 cells), 63% of the BEP2D cells and 70% of the AsbTB2A cells. At first sight, this level of accuracy seems disappointing. However, further scrutiny of the confusion matrix reveals some interesting features. The HPV 16 E7 expressing cells were derived by transduction of the normal human bronchial epithelial cells used for comparison, as were the CDK4-expressing cells. Moreover, the cells were analyzed after expression of these genes for only a few population doublings and thus represent the earliest stages of tumorigenesis. It is perhaps not surprising therefore that some cells retain sufficient "normal" characteristics that they are classified with the normal cells. Conversely, some normal cells were classified as abnormal but almost all of these were mis-identified as either E7-expressing or CDK4-expressing cells. None of the cell cultures used in this study were synchronized, and hence one possible explanation for this observation is that Raman spectroscopy identifies cell cycle-specific features that are present in a proportion of normal cells: this would be consistent with the known cell-cycle effects of the E7 and CDK4 proteins.[14,20]

Similarly, the classification of 18% of the CDK4-expressing cells as E7-expressing cells most likely reflects the biological similarity of the effects of these 2 proteins. CDK4 overexpression leads to pRb phosphorylation.[14] This is equivalent to the major cellular effect of the HPV E7 protein, which binds to and inactivates pRB: this has the same biological effect as pRb phosphorylation, namely, release of E2F and activation of S-phase-associated genes.[20] However, whilst there is overlap between these 2 cell types, the ability of Raman spectroscopy to distinguish between them in most cases indicates the strength of this approach. Biologically, the fact that these cells can be distinguished most likely reflects the known additional non-pRb-dependent effects of the E7 protein.[21]

BEP2D cells were derived by immortalization of bronchial epithelial cells with HPV 18,[16] and AsbTB2A cells are transformed cells that were derived from BEP2D cells by exposure to asbestos, which is a known lung carcinogen.[17] It is of note that our Raman approach discriminates very effectively between normal cells and both BEP2D cells (96%) and TB2A cells (100%). There is, however, some overlap with the E7-expressing and CDK4-expressing cells. It is tempting to speculate that this may reflect pRb pathway defects, which are likely to be present in all of these cells, either through the effects of HPV E7 proteins (E7 cells, BEP2D and AsbTB2A) or overexpression of CDK4 (CDK4 cells). Irrespective of the mechanism involved, these findings indicate that only 4% of the BEP2D cells, and none of the TB2A cells, would have been mis-classified as normal. The overlap between BEP2D and AsbTB2A cells is not unexpected, given that the latter is derived from the former but the correct identification of 63 and 70% of these cells respectively indicates that the effects of asbestos-induced transformation are detectable by Raman spectroscopy.

The aim of this study was to investigate if Raman spectroscopy could be used to identify and potentially grade lung neoplasia in cell samples. Overall, Raman spectroscopy, in combination with the LDA algorithm, was able to identify abnormal cells with a sensitivity of 91% and a specificity of 75%. More specifically, subdivision of the cell types into 3 groups, representing normal cells, cells with extended lifespan (E7 and CDK4 cells) and immortalized/transformed cells (BEP2D and AsbTB2A) shows that Raman spectroscopy identifies cells in these categories correctly with sensitivities of 75, 79 and 87%, and specificities of 91, 85 and 96%, respectively (Table II).

In conclusion, Raman spectroscopy can, with high sensitivity, detect the presence of neoplastic development in lung cells and identify the stage of this development accurately, suggesting that this minimally invasive optical technology has potential for lung cancer diagnosis.

Acknowledgements

The authors thank Dr. Lyndsey Gray and Mr. Dan Smith for their help with cell culture and Dr. Tom Hei for providing the BEP2D and AsbTB2A cell lines.

References

1. Parkin DM, Bray F, Ferlay J, Pisani P. Global cancer statistics, 2002. CA Cancer J Clin 2005;55:74–108.
2. Ferlay J, Autier P, Boniol M, Heanue M, Colombet M, Boyle P. Estimates of the cancer incidence and mortality in Europe in 2006. Ann Oncol 2007;18:581–92.
3. Sant M, Aareleid T, Berrino F, Bielska Lasota M, Carli PM, Faivre J, Grosclaude P, Hedelin G, Matsuda T, Moller H, Moller T, Verdecchia A, et al. EUROCARE-3: survival of cancer patients diagnosed 1990-94—results and commentary. Ann Oncol 2003;14(Suppl 5):v61–v118.
4. Marcus PM, Bergstralh EJ, Zweig MH, Harris A, Offord KP, Fontana RS. Extended lung cancer incidence follow-up in the Mayo Lung Project and overdiagnosis. J Natl Cancer Inst 2006;98:748–56.
5. Ganti AK, Mulshine JL. Lung cancer screening. Oncologist 2006;11:481–7.
6. Stone N, Kendall C, Smith J, Crow P, Barr H. Raman spectroscopy for identification of epithelial cancers. Faraday Discuss 2004;126:141–57; discussion 69–83.
7. Crow P, Stone N, Kendall CA, Uff JS, Farmer JA, Barr H, Wright MP. The use of Raman spectroscopy to identify and grade prostatic adenocarcinoma in vitro. Br J Cancer 2003;89:106–8.
8. Huang Z, McWilliams A, Lui H, McLean DI, Lam S, Zeng H. Near-infrared Raman spectroscopy for optical diagnosis of lung cancer. Int J Cancer 2003;107:1047–52.
9. Koljenovic S, Bakker Schut TC, van Meerbeeck JP, Maat AP, Burgers SA, Zondervan PE, Kros JM, Puppels GJ. Raman microspectroscopic mapping studies of human bronchial tissue. J Biomed Opt 2004;9:1187–97.
10. Yamazaki H, Kaminaka S, Kohda E, Mukai M, Hamaguchi HO. The diagnosis of lung cancer using 1064-nm excited near-infrared multichannel Raman spectroscopy. Radiat Med 2003;21:1–6.
11. Short MA, Lam S, McWilliams A, Zhao JH, Lui H, Zeng HS. Development and preliminary results of an endoscopic Raman probe for potential in vivo diagnosis of lung cancers. Opt Lett 2008;33:711–13.
12. Bakker Schut TC, Puppels GJ, Kraan YM, Greve J, van der Maas LL, Figdor CG. Intracellular carotenoid levels measured by Raman microspectroscopy: comparison of lymphocytes from lung cancer patients and healthy individuals. Int J Cancer 1997;74:20–5.
13. Jess PR, Smith DD, Mazilu M, Dholakia K, Riches AC, Herrington CS. Early detection of cervical neoplasia by Raman spectroscopy. Int J Cancer 2007;121:2723–8.
14. Morris M, Hepburn P, Wynford-Thomas D. Sequential extension of proliferative lifespan in human fibroblasts induced by over-expression of CDK4 or 6 and loss of p53 function. Oncogene 2002;21:4277–88.
15. Gray LJ, Bjelogrlic P, Appleyard VC, Thompson AM, Jolly CE, Lain S, Herrington CS. Selective induction of apoptosis by leptomycin B in keratinocytes expressing HPV oncogenes. Int J Cancer 2007;120:2317–24.
16. Willey JC, Broussoud A, Sleemi A, Bennett WP, Cerutti P, Harris CC. Immortalization of normal human bronchial epithelial cells by human papillomaviruses 16 or 18. Cancer Res 1991;51:5370–7.
17. Zhao YL, Piao CQ, Wu LJ, Suzuki M, Hei TK. Differentially expressed genes in asbestos-induced tumorigenic human bronchial epithelial cells: implication for mechanism. Carcinogenesis 2000;21:2005–10.
18. Tabaksblat R, Meier RJ, Kip BJ. Confocal Raman microspectroscopy—theory and application to thin polymer samples. Appl Spectrosc 1992;46:60–8.
19. Ripley B. Pattern recognition and neural networks. Cambridge: Cambridge University Press, 1996.
20. Gray L, Jolly C, Herrington CS. Human papillomaviruses and their effects on cell cycle control and apoptosis. In: Digard P, Nash AA, Randall RE, eds. Society for general microbiology symposium 64: molecular pathogenesis of virus infections. Cambridge: Cambridge University Press, 2005. 235–51.
21. Munger K, Basile JR, Duensing S, Eichten A, Gonzalez SL, Grace M, Zacny VL. Biological activities and molecular targets of the human papillomavirus E7 oncoprotein. Oncogene 2001;20:7888–98.